

Supplementary Information (SI)

Self-quenched Ferrocenyl Diketopyrrolopyrrole Organic Nanoparticles with Amplifying Photothermal Effect for Cancer Therapy

Pingping Liang,^a Qianyun Tang,^a Yu Cai,^a Gongyuan Liu,^a Weili Si,^a Jinjun Shao,^a Wei Huang,^{*a} Qi Zhang,^{*b} Xiaochen Dong^{*a}

^aKey Laboratory of Flexible Electronics (KLOFE) & Institute of Advanced Materials (IAM), Jiangsu National Synergetic Innovation Center for Advanced Materials (SICAM), Nanjing Tech University (NanjingTech), 30 South Puzhu Road, Nanjing 211816, China.

E-mail: iamxcdong@njtech.edu.cn; iamwhuang@njtech.edu.cn

^bSchool of Pharmaceutical Sciences, Nanjing Tech University (NanjingTech), Nanjing China.

E-mail: zhangqi@njtech.edu.cn

Supplementary Information (SI)

Table of Contents

Experimental Section	S4
Materials	S4
Characterization	S4
Synthesis of DPP	S4
Synthesis of DPPBr	S5
Synthesis of DPP-Fc	S5
Synthesis of DPPCN-Fc	S6
Preparation of DPPCN-Fc NPs	S6
Characterization and Morphology Analysis	S6
Measurement of Photothermal Performance.....	S7
Photo-stability of DPPCN-Fc NPs.....	S7
Photothermal Conversion (PTC) Efficiency	S7
Cell Culture and Incubation Conditions.....	S8
<i>In vitro</i> Cell Cytotoxicity	S9
<i>In vitro</i> Photothermal Cancer Cell Killing	S9
<i>In vitro</i> Cellular Uptake of DPPCN-Fc NPs.....	S10
Animals and Tumor Model.....	S10
Photoacoustic Imaging.....	S10
<i>In vivo</i> Photothermal Therapy	S10
Histology Sample Preparation	S11
Supplementary References	S11
Supplementary Figures	S12

Supplementary Information (SI)

Figure S1. ^1H NMR Spectrum of DPP-Fc	S13
Figure S2. ^{13}C NMR Spectrum of DPP-Fc	S13
Figure S3. ^1H NMR Spectrum of DPPCN-Fc	S14
Figure S4. ^{13}C NMR Spectrum of DPPCN-Fc	S15
Figure S5. MALDI-TOF-MS of DPPCN-Fc	S16
Figure S6. Molar extinction coefficient	S17
Figure S7. The dispersion stability of DPPCN-Fc NPs	S18
Figure S8. Characterization of quenching mechanism	S19
Figure S9. Reactive oxygen species generation	S20
Figure S10. Cell viability of A2780 cells.....	S21
Figure S11. H&E stained of major organs	S22

Supplementary Information (SI)

Experimental Section

Materials

All commercially available materials and chemicals were purchased from Sigma-Aldrich and used without further purification unless otherwise explanations. Tetracyanoethylene was purchased from Alfa Aesar (China) chemicals Co. Ltd. 3,4,5-trimethyl-2-thiazolyl)-2,5-diphenyl-2-H-tetrazolium bromide (MTT) and Fetal bovine serum were purchased from GIBCO. 4',6-diamidino-2-phenylindole (DAPI) were purchased from Institute of Biochemistry and Cell Biology, SIBS, CAS (China).

Characterization

Intermediate products and DPPCN-Fc NPs were characterized via ^1H NMR, ^{13}C NMR spectra (Bruker DRX NMR spectrometer), UV-vis-NIR spectrophotometer (Shimadzu, Japan), TCSPC equipment (FLS980, England), transmission electron microscopy (TEM, JEM-2010FEF), scanning electron microscope (SEM) and dynamic light scattering (DLS, Malvern Zeta Sizer). Other apparatus were confocal fluorescence microscope (Olympus IX 70), simulated sunlight xenon lamp light source system (Beijing Taught Jin Yuan Technology Co., Ltd), optical fiber coupled 730 nm diode-laser, IR thermal camera (FLIR Systems, Inc., Wilsonville, OR, USA) and multispectral photoacoustic tomography (MSOT) system. The experiment was performed in strict accordance with National Institutes of Health (NIH) guidelines for the care and use of laboratory animals (NIH Publication no. 85-23 Rev. 1985). In addition, all procedures were approved by Research Center for Laboratory Animals of Yangzhou University of Traditional Chinese Medicine (Yangzhou, China). For the protection of human subjects, the investigators adhered to the policies of applicable law.

Synthesis of DPP

Diketopyrrolopyrrole nucleus (5.36 g, 20 mmol), 1-Bromo-iso-octane (11.59 g, 60 mmol) and potassium carbonate (8.29 g, 60 mmol) were dissolved in N, N-dimethyl formamide

Supplementary Information (SI)

(400 mL) and stirred at 120 °C for 24 hours. The solvent was removed. Then washed and dried the crude product. At last, the resulted residue was purified by chromatography on a silica column (PE/DCM, V/V=1:6) to obtain DPP (5.10 g, yield: 50%). ¹H NMR (300 MHz, CDCl₃) δ 8.33 (d, *J* = 3.6 Hz, 2H), 7.61 (s, 2H), 6.85 (m, 2H), 4.04 (d, *J* = 7.3 Hz, 4H), 1.76 (s, 2H), 1.54 (s, 4H), 1.40 – 1.18 (m, 16H), 1.02 – 0.81 (m, 10H). ¹³C NMR (75 MHz, CDCl₃) δ ¹³C NMR (75 MHz, CDCl₃) δ 145.91, 120.87, 114.97, 48.02, 40.99, 30.60, 28.71, 23.78, 22.99, 15.65, 10.56.

Synthesis of DPPBr

In a 100 mL round bottom flask, diketopyrrolopyrrole (DPP) (516.81 mg, 1.02 mmol) was dissolved in chloroform (30 mL) at room temperature. Then the mixture was stirred for 10 min and the N-Bromosuccinimide (NBS) (396.90 mg, 2.23 mmol) was quickly added in the dark. The reaction mixture was stirred at room temperature for 4 hours. After completion of the reaction, the mixture was washed with saline water for three times. The organic layer was extracted with dichloromethane, dried over with anhydrous sodium sulfate, and solvent was removed by rotary evaporation. At last, the product was purified by chromatography (silica gel, dichloromethane/petroleum ether, 5:1,) to yield DPPBr (540 mg, yield: 80%) as a purple solid. ¹H NMR (300 MHz, CDCl₃) δ 8.30 (d, *J* = 3.6 Hz, 2H), 6.62 (d, *J* = 3.6 Hz, 2H), 3.64 (d, *J* = 213.5, 198.7 Hz, 4H), 1.82 – 1.63 (m, 2H), 1.39 – 1.05 (m, 16H), 0.91 (d, *J* = 13.8, 6.7 Hz, 6H), 0.80 (t, 6H). ¹³C NMR (75 MHz, CDCl₃) δ 160.93, 146.06, 132.44, 126.27, 122.26, 115.53, 79.01, 46.28, 40.08, 30.55, 28.74, 23.48, 23.18, 14.06, 10.68.

Synthesis of DPP-Fc

In a 50 mL round-bottomed flask, DPPBr (205.98 mg, 0.31 mmol) and ethynylferrocene (128.43 mg, 0.62 mmol) were dissolved in triethylamine (6 mL) mixed with dry toluene (10 mL). The reaction mixture was degassed with nitrogen for 15 min, then PdCl₂(PPh₃)₂ (20.06 mg, 0.03 mmol), PPh₃ (15.74 mg, 0.06 mmol), and CuI (5.71 mg, 0.03 mmol) were added. And the reaction mixture was stirred at 80 °C for 12 h. At last, the reaction mixture was cooled to room temperature. The solvent was removed by rotary evaporation, and the product was purified by chromatography (silica gel, dichloromethane/hexane, 1:3) to yield DPP-Fc

Supplementary Information (SI)

(233 mg, yield: 83%) as bluish violet solid. ^1H NMR (500 MHz, CDCl_3) δ 8.40 (d, 2H), 7.26 (s, 2H), 4.54 (s, 4H), 4.30 (d, 4H), 4.06 (s, 4H), 4.08 (s, 2H), 1.84 (s, 4H), 1.55 (s, 6H), 1.36 (s, 22H), 0.88 (s, 6H). ^{13}C NMR (75 MHz, CDCl_3) δ 162.09, 144.51, 139.89, 132.71, 128.55, 121.67, 117.67, 77.00, 76.05, 71.68, 69.93, 67.54, 46.33, 40.13, 31.53, 30.78, 29.69, 28.58, 27.97, 27.15, 22.99 14.08 (Figure S1 and Figure S2).

Synthesis of DPPCN-Fc

In a 50 mL round-bottomed flask, DPP-Fc (90.87 mg, 0.1 mmol) and TCNE (25.62 mg, 0.2 mmol) were dissolved in dichloromethane (20 mL) under nitrogen and the reaction mixture was stirred at room temperature for 6 h. Upon completion of the reaction, the solvent was removed through rotary evaporation, and the product was purified by chromatography (silica gel, dichloromethane/hexane, 1:2) to yield DPPCN-Fc (112 mg, yield: 96%) as a dark green solid. ^1H NMR (500 MHz, CDCl_3) δ 8.50 (s, 2 H), 7.35 (s, 2H), 5.64 (s, 2H), 5.04 (s, 2H), 4.87 (s, 2H), 4.51 (s, 2H), 4.35 (s, 2H), 4.08 (s, 2H), 3.95 (s, 2H), 1.56 (m, 4H), 1.31 (s, 28H), 0.87 (s, 6H). ^{13}C NMR (126 MHz, CDCl_3) δ 168.93, 160.31, 150.25, 139.45, 136.47, 135.83, 133.95, 133.18, 132.42, 124.87, 123.91, 123.42, 113.54, 112.50, 79.51, 76.83, 75.57, 75.38, 72.64, 72.19, 71.46, 71.19, 46.89, 44.56, 39.82, 39.34, 30.26, 29.68, 29.18, 28.58, 22.93, 22.93, 13.96 (Figure S3 and Figure S4). MALDI-TOF-Mass Spectrum of DPPCN-Fc (Figure S5).

Preparation of DPPCN-Fc NPs

DPPCN-Fc NPs were obtained by the re-precipitation method. 400 μL of a 2 mg/mL DPPCN-Fc (dissolved in THF) solution were added drop-wise into 10 mL of deionized water by a microsyringe at room temperature with magnetic stirring. During this process, the DPPCN-Fc molecules self-assembled into NPs through strong π - π stacking and hydrophobic interactions. After stirring for 10 min, the THF in the solution was removed by continuous bubbling nitrogen at room temperature.

Characterization and Morphology Analysis

Supplementary Information (SI)

The size and microstructure of as-prepared nanoparticles were characterized by TEM and SEM. TEM samples were acquired by drop-casting a concentrated solution of FDPPCN-Fc NPs on copper grids using a JEOL JEM-1011 microscope operated at 100 kV accelerating voltage. SEM samples were acquired by depositing a concentrated solution of DPPCN-Fc NPs on a silicon substrate and operated by a FEI quanta 200F microscope. The particle sizes of the DPPCN-Fc NPs were determined by dynamic light scattering (DLS) measurements on a Malvern Zetasizer (Nano-ZS, Malvern Instruments, Ltd., UK) instrument. The ultraviolet-visible (UV-vis) data were recorded by an UV-3600 UV-vis-NIR spectrophotometer (Shimadzu, Japan), using quartz cuvettes with an optical path-length of 1 cm in the wavelength range of 300–900 nm. The fluorescence lifetime and fluorescence spectrum were recorded by a TCSPC equipment (FLS980, England), using quartz cuvettes with an optical path-length of 1 cm in the wavelength range of 400-900 nm.

Measurement of Photothermal Performance

Photothermal performance of the samples was evaluated by adopting a similar ways as previously,¹⁻³ Aqueous solutions of DPPCN-Fc NPs (2 mL) in a quartz cuvette were exposed to the laser (wavelength, 730 nm) at different concentrations (0, 20, 40, 60, 80, 100 µg/mL) and different power densities (0.2, 0.4, 0.6, 0.8 and 1.0 W/cm²) for 10 min with IR thermal camera and BMIR software to monitor their temperature changes and thermal images.

Photo-stability of DPPCN-Fc NPs

To explore photo-stability, the UV-vis-NIR spectrum of the DPPCN-Fc NPs aqueous dispersion before and after four cycles of heating (laser on: 5 min) and cooling (laser off: 5 min) under 730 nm laser irradiation were recorded.

Photothermal Conversion (PTC) Efficiency

For measuring the PTC efficiency of DPPCN-Fc NPs, a quartz cuvette with 1 cm path length, filled with 2 mL of aqueous solution of DPPCN-Fc NPs was irradiated with 730 nm laser (1.3 W/cm²) for 10 min. The laser was shut off when the temperature reached a plateau. And

Supplementary Information (SI)

the temperature was recorded by IR thermal camera one time per 20 s for the whole process. Deionized water of the same volume was used as a contrast.⁴⁻⁶

The PTC efficiency was calculated by equation (1)

$$\eta = \frac{hS (T_{\max} - T_{\text{surr}}) - Q_0}{I (1 - 10^{-A730})} \quad (1)$$

Where h represents the heat transfer coefficient, S represents the sample container surface area, T_{\max} represents the steady-state maximum temperature, T_{surr} represents the ambient room temperature, Q_0 represents the energy input by the same solvent without NPs in the same quartz cuvette after same laser irradiation.

In order to calculate the hS , θ was introduced, which was defined as follow ratio:

$$\theta = \frac{T - T_{\text{surr}}}{T_{\max} - T_{\text{surr}}} \quad (2)$$

so the value of hS was calculated by the follow equation:

$$\tau_s = \frac{C_d m_d}{hS} \quad (3)$$

Where τ_s represents the characteristic thermal time constant, and the heat capacity c_d of water was about $4.2 \text{ J g}^{-1} \text{ K}^{-1}$, m_d represented the mass of the solution (g). Q_0 was calculated using the following equation:

$$Q_0 = hS (T_{\max} - T_{\text{surr}}) \quad (4)$$

Cell Culture and Incubation Conditions

HeLa cancer cells were obtained from the Institute of Biochemistry and Cell Biology, SIBS, CAS (China) and cultured in fresh Dulbecco's Modified Eagle's Medium (DMEM) containing 10% inactivated fetal bovine serum (FBS) and 1% (penicillin and streptomycin) under a humidified atmosphere with 5% CO_2 and 95% air at $37 \text{ }^\circ\text{C}$. The culture medium

Supplementary Information (SI)

were replaced into fresh medium about every two days and were split about every 3 days before they reached 90% confluence.

***In vitro* Cell Cytotoxicity**

The cytotoxicity of DPPCN-Fc NPs in dark was verified by standard MTT assay. HeLa and A2780 cells were seeded into two 96-well plates at a density of about 1×10^5 cells per well in 200 μL fresh complement medium and incubated the cells for 24 hours in a humidified atmosphere. After that, the medium was replaced by the fresh complement medium with various concentrations of DPPCN-Fc NPs (0, 20, 40, 60, 80, 100, 120 $\mu\text{g}/\text{mL}$) for 24 and 48 h under dark conditions in the incubator (the number of the replication well is five). After that, the MTT solution (20 μL , 5 mg/mL) was added to each well and incubated for another 4 h. Then DMSO (150 μL) was added to dissolve the purple precipitate. The absorption intensity was measured at the optical densities (O.D) of 492 nm with a microplate reader. The mean cell viability and standard deviation for the parallel five wells for each concentration were calculated. Cell viability values were calculated by the following formula: Cell viability (%) = absorbance of experimental group/ the absorbance of control group $\times 100\%$.

***In vitro* Photothermal Cancer Cell Killing**

For assessment photothermal cancer cell killing *in vitro*, HeLa cells were seeded into two 96-well plates at a density of about 1×10^5 cells per well in 200 μL fresh complement medium and incubated the cells for 24 hours in a humidified atmosphere. After that, the medium was replaced by the fresh complement medium with various concentrations of DPPCN-Fc NPs (0, 4, 8, 12, 16, 20, 24 and 28 $\mu\text{g}/\text{mL}$) for 24 h under the dark condition in the incubator (the number of the replication well is five) and then one of the two plates was still kept in dark and the other was irradiated with a 730 nm laser (1 W / cm^2). For each well the irradiation time was 3 minutes. Then the cells were incubated for an additional 12 hours. After that, the MTT solution (20 μL , 5 mg/mL) was added to each well and incubated for another 4 h. Then DMSO (150 μL) was added to dissolve the purple precipitate. The absorption intensity was

Supplementary Information (SI)

measured at the optical densities (O.D) of 492 nm with a microplate reader. The mean cell viability and standard deviation for the parallel five wells for each concentration were calculated. Cell viability values were also calculated by the following formula: Cell viability (%) = absorbance of experimental group/the absorbance of control group $\times 100\%$.

***In vitro* Cellular Uptake of DPPCN-Fc NPs**

For the cell imaging, HeLa cells were seeded into a confocal culture plate in 2 mL fresh complement medium and incubated the cells for 24 hours in a humidified atmosphere. After that, the medium was replaced by the fresh complement medium of 80 $\mu\text{g}/\text{mL}$ DPPCN-Fc NPs aqueous solution for 24 hours under dark conditions in the incubator. The cells were stained with 4',6-diamidino-2-phenylindole (DAPI) at room temperature for 3 min before the observation. The image was monitored by a laser scanning up-conversion luminescence microscope equipped (Olympus IX 70).

Animals and Tumor Model

Based on the *in vitro* experiments. We next explored the DPPCN-Fc NPs for the experiments *in vivo*. 20 nude mice (five weeks aged, 18-20 g weight) were obtained from Comparative Medicine Centre of Yangzhou University. The HeLa tumors were generated by the left front leg subcutaneous injection with 200 μL of PBS containing 4×10^6 cells. All the mice were carefully arranged in ventilated animal rooms in the cages with free access to a commercial laboratory complete food and water. *In vivo* experiments were carried out when the tumor volumes approached 100-150 mm^3 .

Photoacoustic Imaging

For *in vitro* PA imaging, DPPCN-Fc NPs in deionized water with various concentrations (0, 5, 10, 20, 40 and 80 $\mu\text{g}/\text{mL}$) were scanned with the multispectral photoacoustic tomography (MSOT) system. For *in vivo* PA imaging, the mice were anaesthetized with chloral hydrate solution. After the intravenous injection of DPPCN-Fc NPs, the contrast data at various time points (0, 2, 4, 6, 8 and 10 h) were obtained using the MSOT system with excitation

Supplementary Information (SI)

wavelengths of 730 nm.

***In vivo* Photothermal Therapy**

The HeLa tumors bearing mice were divided into four groups (saline only, saline with laser, NPs only and NPs with laser, n=5/group). When the tumor volume was about 100-150 mm³, mice in the saline and saline with laser group were injected with normal saline (100 μL). Mice in the NPs only and NPs with laser group were injected with PBS containing DPPCN-Fc NPs (100 μL, pH = 7.4). After 6 h of injection, the solid tumors of the saline with laser and NPs with laser groups were irradiated for 8 min with an optical fiber coupled 730 nm diode-laser (power density: 1 W/cm², laser beam diameter: 5 mm) The thermal images were taken by an infrared thermal imaging camera. The body weight and tumor volumes of each group were recorded by a digital scale and caliper for 18 days (one time every two days). The tumor sizes were calculated by formula of length × width × width/2.

Histology Sample Preparation

After treatment of 18 days, all mice were killed to harvest the tumors and major organs such as heart, liver, lung, spleen, and kidney for histological analysis. The isolated test specimens were fixed in 10% neutral buffered formalin solution for 24 hours at the room temperature and embedded in paraffin for haematoxylin and eosin (H&E) staining. Finally, the slices were observed under an optical microscopy.

References:

- (1) Xiao, Z.; Xu, C.; Jiang, X.; Zhang, W.; Peng, Y.; Zou, R.; Huang, X.; Liu, Q.; Qin, Z.; Hu, J., Hydrophilic bismuth sulfur nanoflower superstructures with an improved photothermal efficiency for ablation of cancer cells. *Nano Res.*, 1-14.
- (2) Sun, X.; Wang, C.; Gao, M.; Hu, A.; Liu, Z., Remotely Controlled Red Blood Cell Carriers for Cancer Targeting and Near - Infrared Light - Triggered Drug Release in Combined Photothermal–Chemotherapy. *Adv. Funct. Mater.* **2015**, *25*, 2386-2394.
- (3) Lin, C. T.; Lin, I.; Sung, S. Y.; Su, Y. L.; Huang, Y. F.; Chiang, C. S.; Hu, S. H., Dual - Targeted Photopenetrative Delivery of Multiple Micelles/Hydrophobic Drugs by a Nanopea for Enhanced Tumor Therapy. *Adv. Funct. Mater.* **2016**.

Supplementary Information (SI)

(4) Ghosh, S.; Avellini, T.; Petrelli, A.; Kriegel, I.; Gaspari, R.; Almeida, G.; Bertoni, G.; Cavalli, A.; Scotognella, F.; Pellegrino, T., Colloidal CuFeS₂ Nanocrystals: Intermediate Fe d-Band Leads to High Photothermal Conversion Efficiency. *Chem. Mater.* **2016**.

(5) Tian, Q.; Jiang, F.; Zou, R.; Liu, Q.; Chen, Z.; Zhu, M.; Yang, S.; Wang, J.; Wang, J.; Hu, J., Hydrophilic Cu₉S₅ nanocrystals: A photothermal agent with a 25.7% heat conversion efficiency for photothermal ablation of cancer cells *in vivo*. *ACS nano* **2011**, *5*, 9761-9771.

(6) Wang, J.; Yan, R.; Guo, F.; Yu, M.; Tan, F.; Li, N., Targeted lipid-polyaniline hybrid nanoparticles for photoacoustic imaging guided photothermal therapy of cancer. *Nanotechnol.* **2016**, *27*, 285102.

Supplementary Figures

¹H NMR Spectrum of DPP-Fc

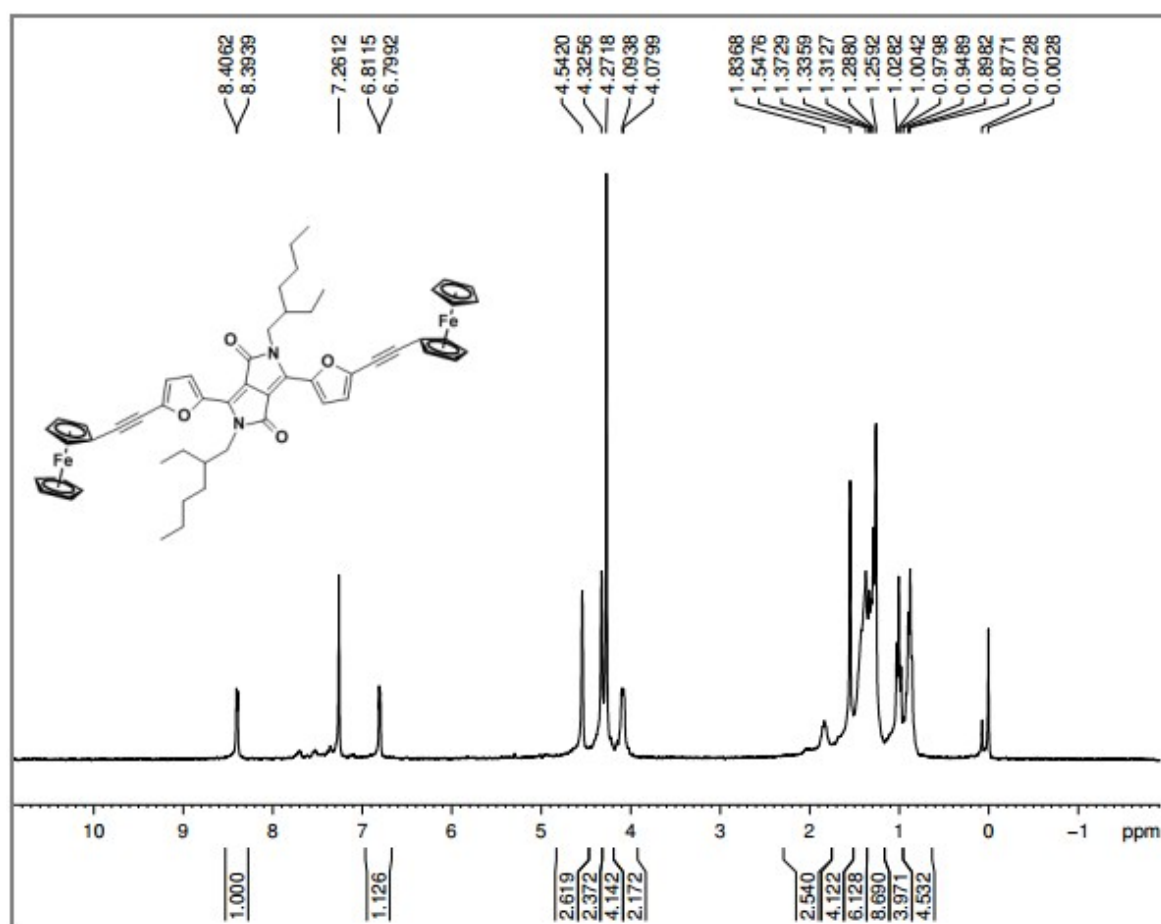


Figure S1. ¹H NMR Spectrum of DPP-Fc.

Supplementary Information (SI)

^{13}C NMR Spectrum of DPP-Fc

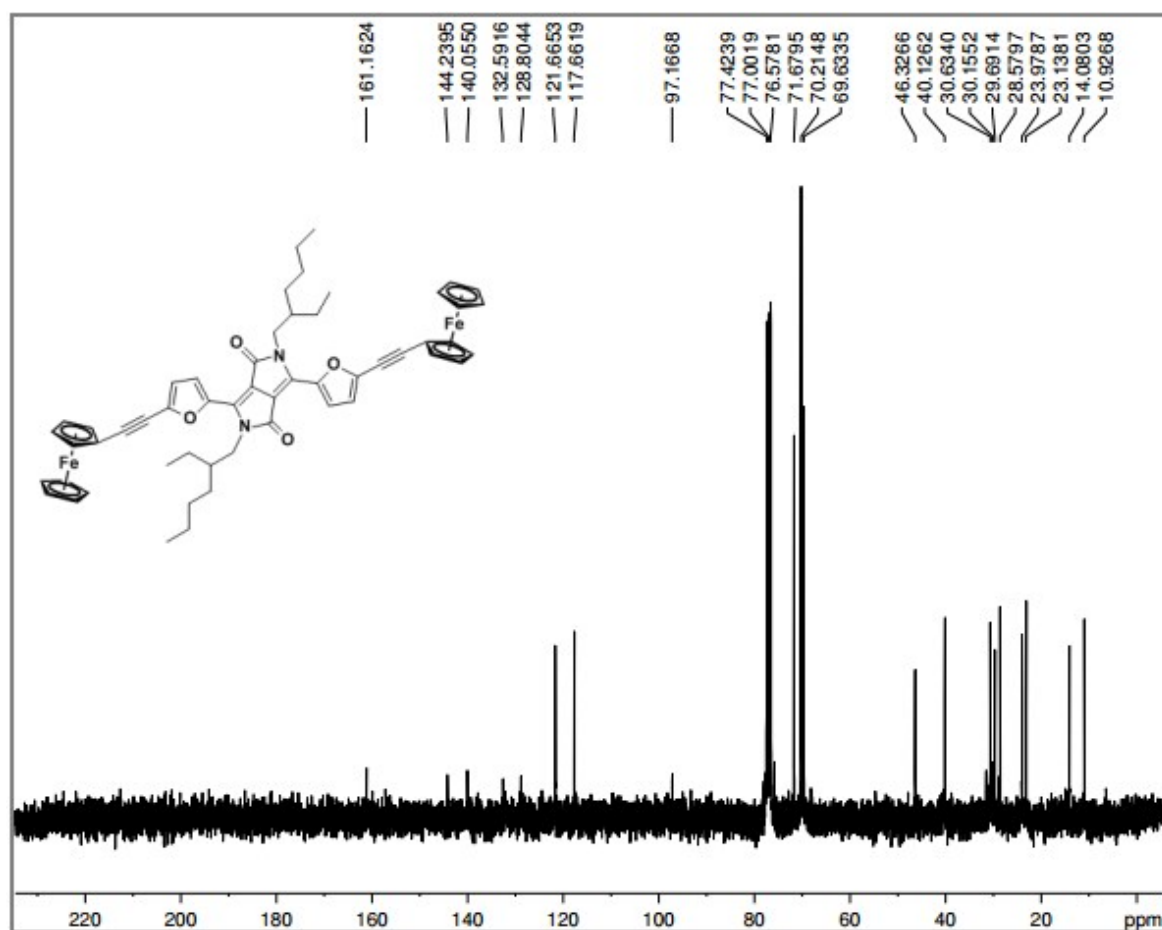


Figure S2. ^{13}C NMR Spectrum of DPP-Fc.

Supplementary Information (SI)

^1H NMR Spectrum of DPPCN-Fc

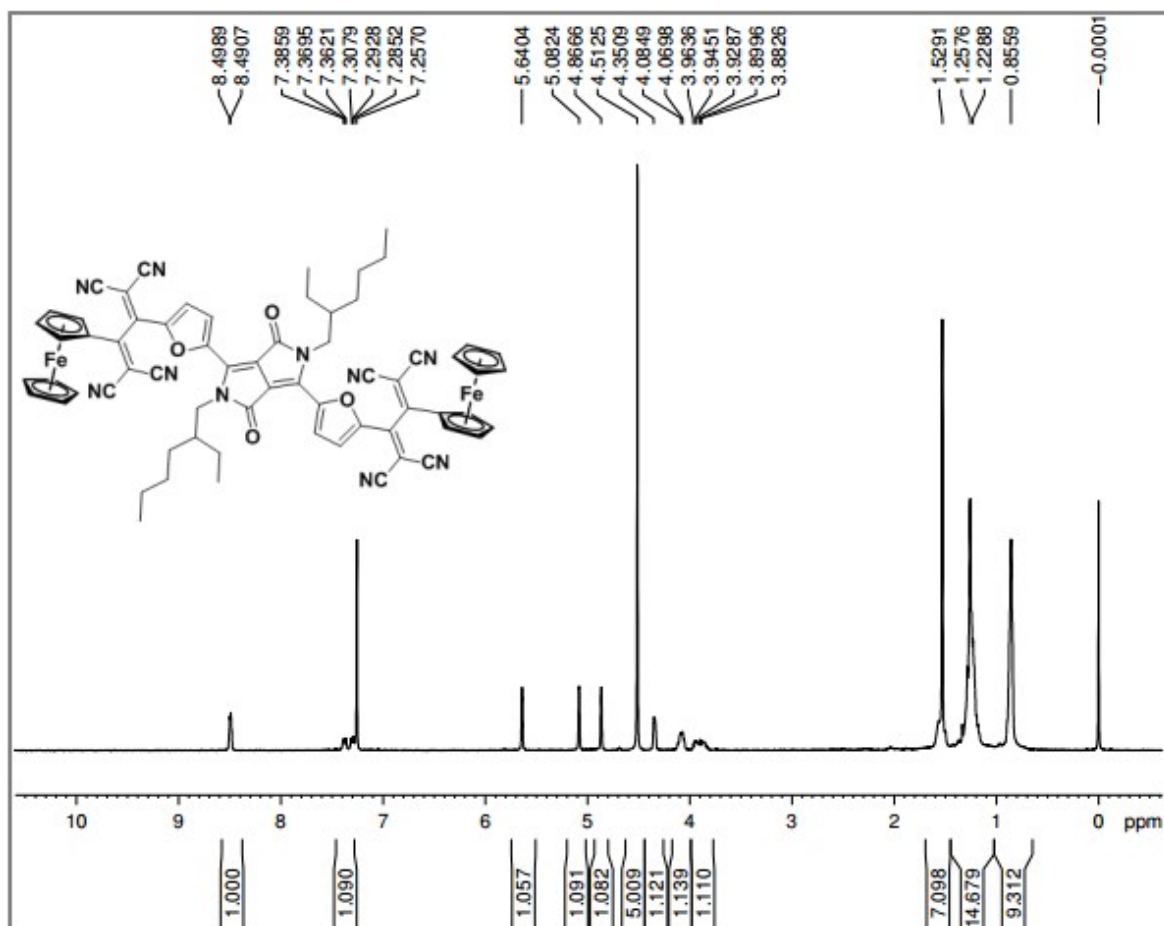


Figure S3. ^1H NMR Spectrum of DPPCN-Fc.

Supplementary Information (SI)

^{13}C NMR Spectrum of DPPCN-Fc

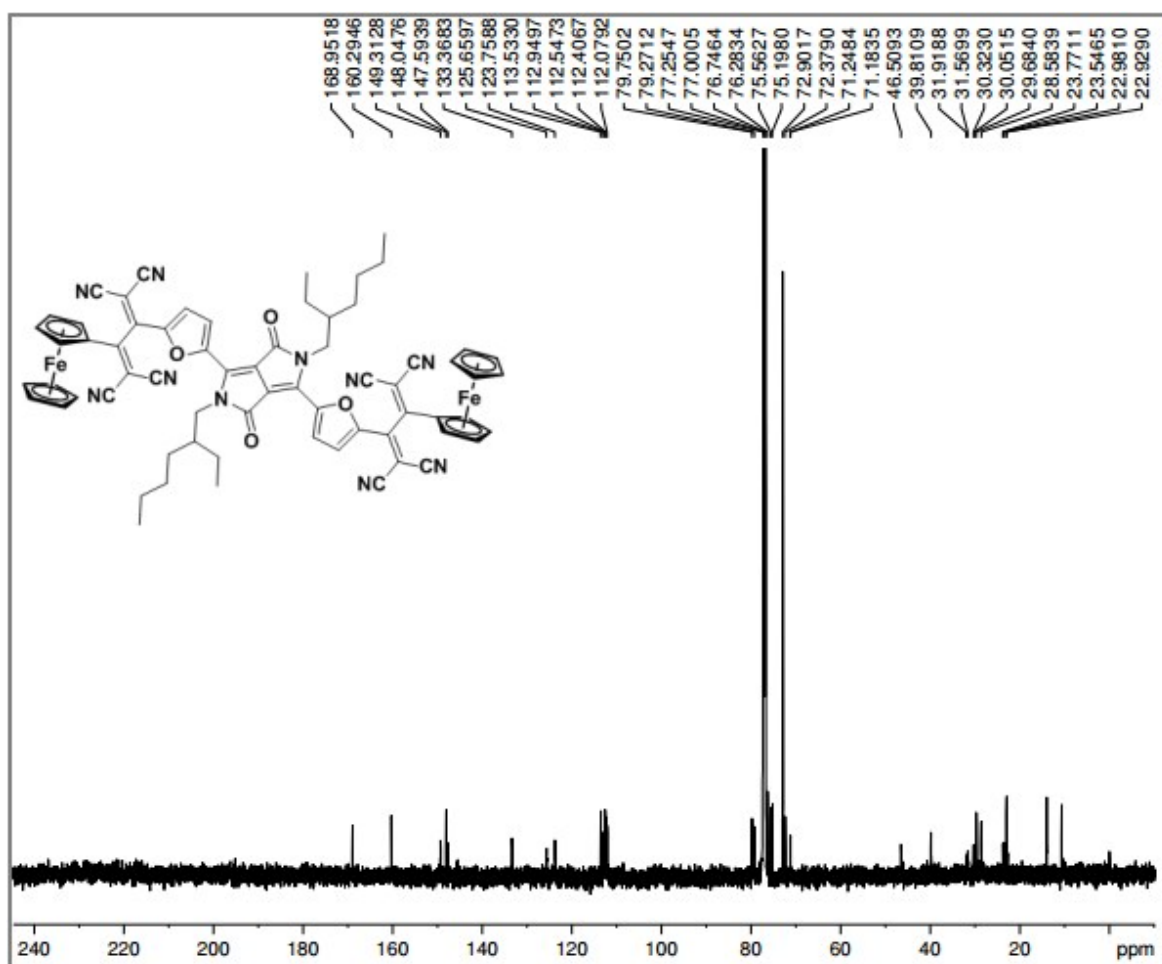


Figure S4. ^{13}C NMR Spectrum of DPPCN-Fc.

Supplementary Information (SI)

MALDI-TOF-Mass Spectrum of DPPCN-Fc.

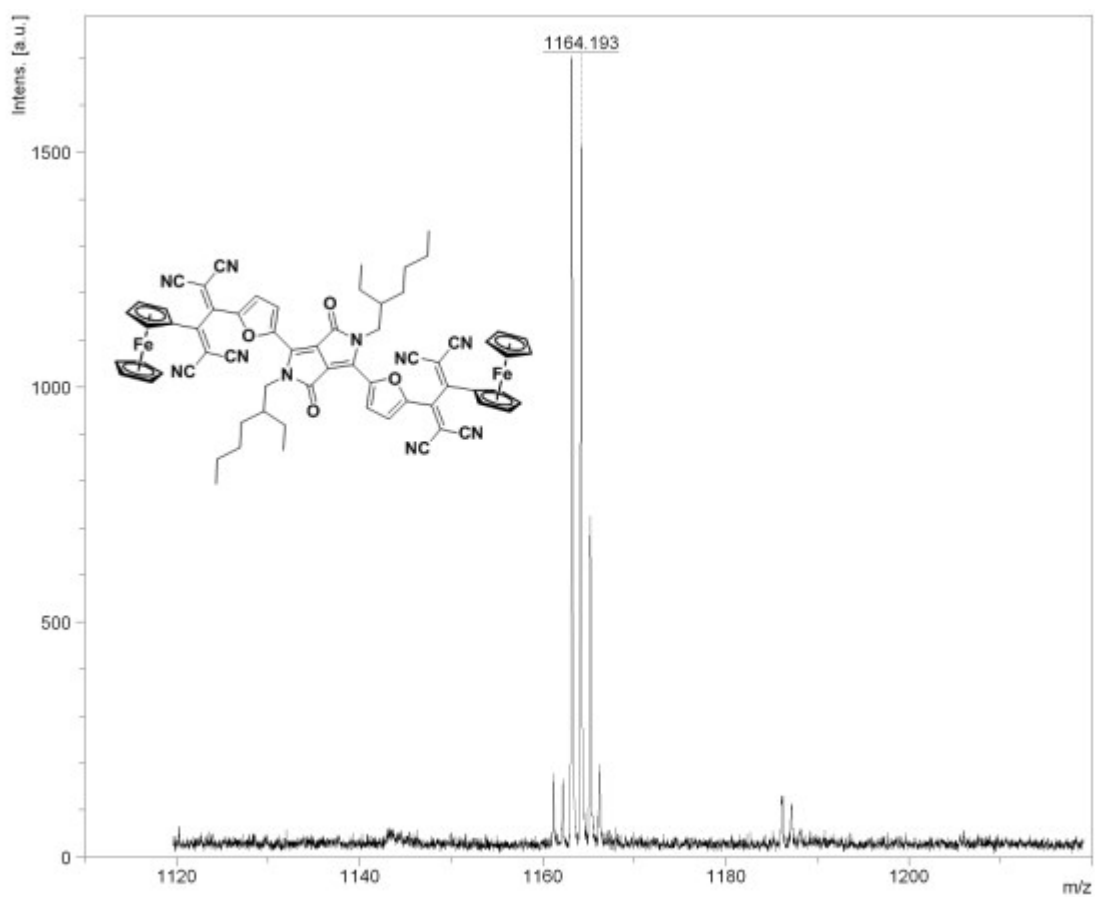


Figure S5. MALDI-TOF-MS of DPPCN-Fc.

Supplementary Information (SI)

Molar extinction coefficient

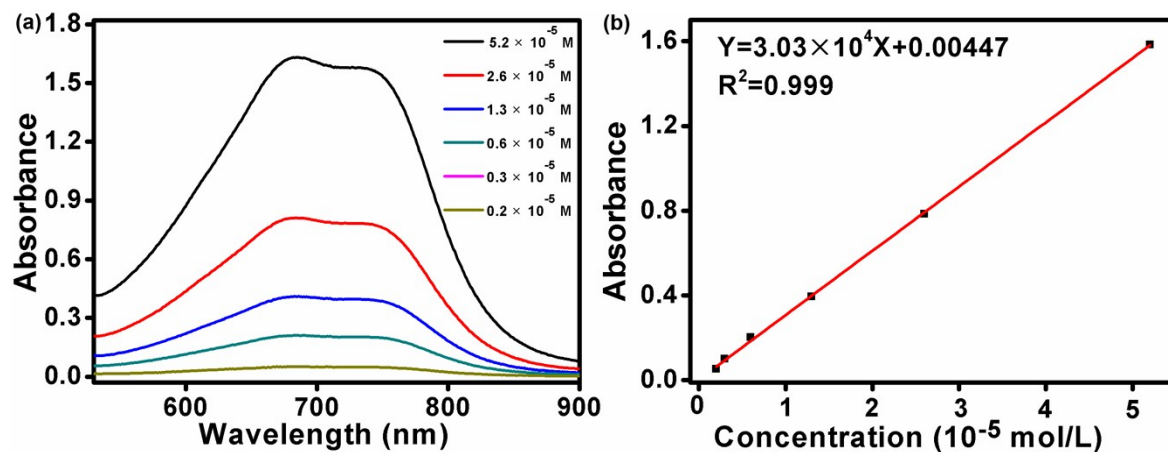


Figure S6. (a) Absorption curves of DPPCN-Fc NPs aqueous solution at different concentrations. (b) Linear absorbance versus concentration obtained from (a).

Supplementary Information (SI)

The dispersion stability of DPPCN-Fc NPs

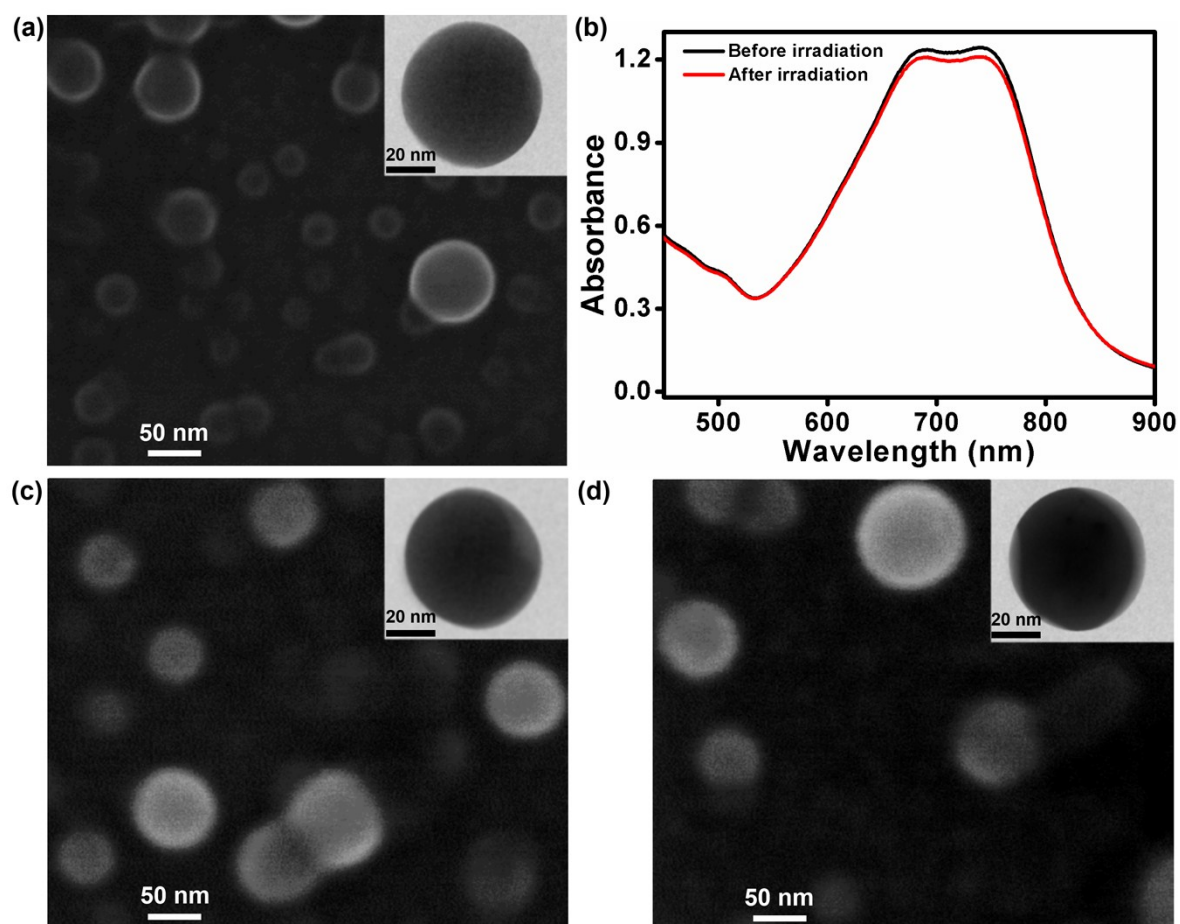


Figure S7. (a) SEM image of DPPCN-Fc NPs. Inset: TEM image of a single DPPCN-Fc NP (in water, after irradiation). (b) UV-vis-NIR absorbance spectra of DPPCN-Fc NPs before /after laser irradiation (in PBS, 730 nm, 1.0 W/cm², 20 min). (c,d) SEM image of DPPCN-Fc NPs. Inset: TEM image of a single DPPCN-Fc NP (in PBS, before/after irradiation, respectively).

Characterization of quenching mechanism

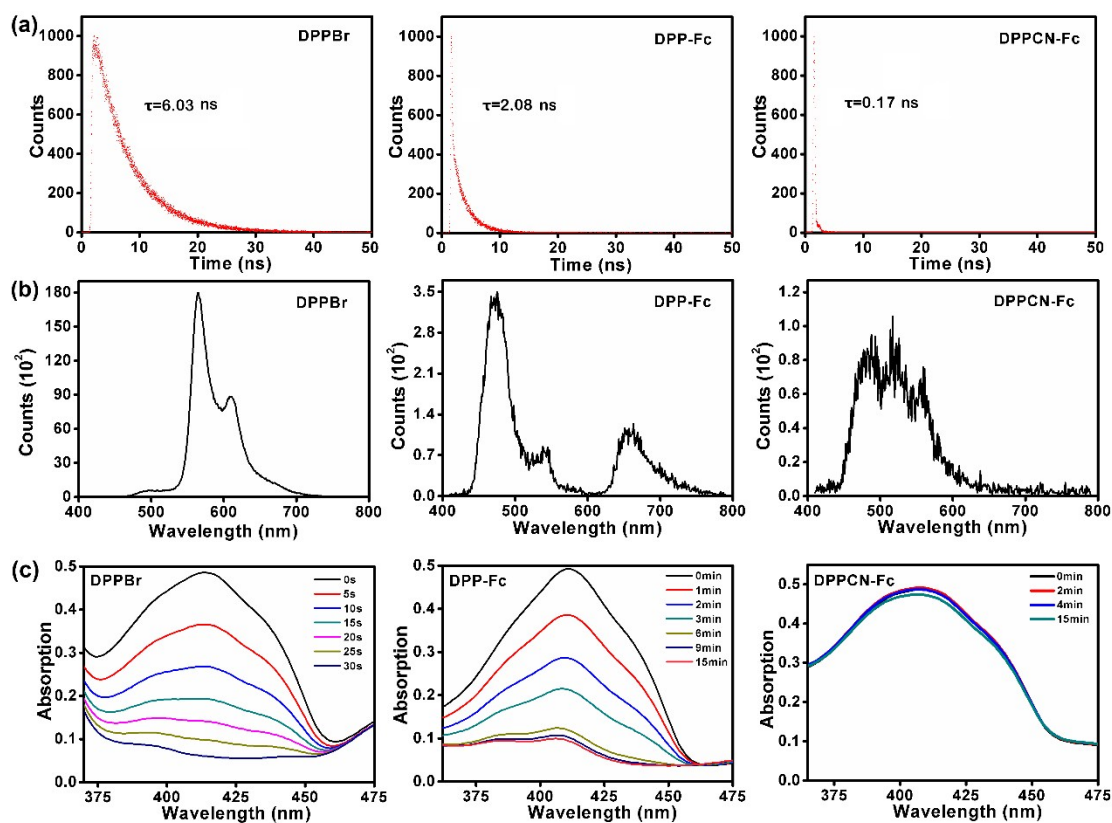


Figure S8. (a, b) Fluorescence decay lifetime and spectra measurement of DPPBr, DPP-Fc and DPPCN-Fc in DCM ($C=1 \times 10^{-5}$ M, 20°C). (c) Absorption spectra at 416 nm of DPPBr, DPP-Fc and DPPCN-Fc (10^{-5} M) mixed with DPBF (10^{-5} M) under illumination in DCM vs time.

Supplementary Information (SI)

Reactive oxygen species generation

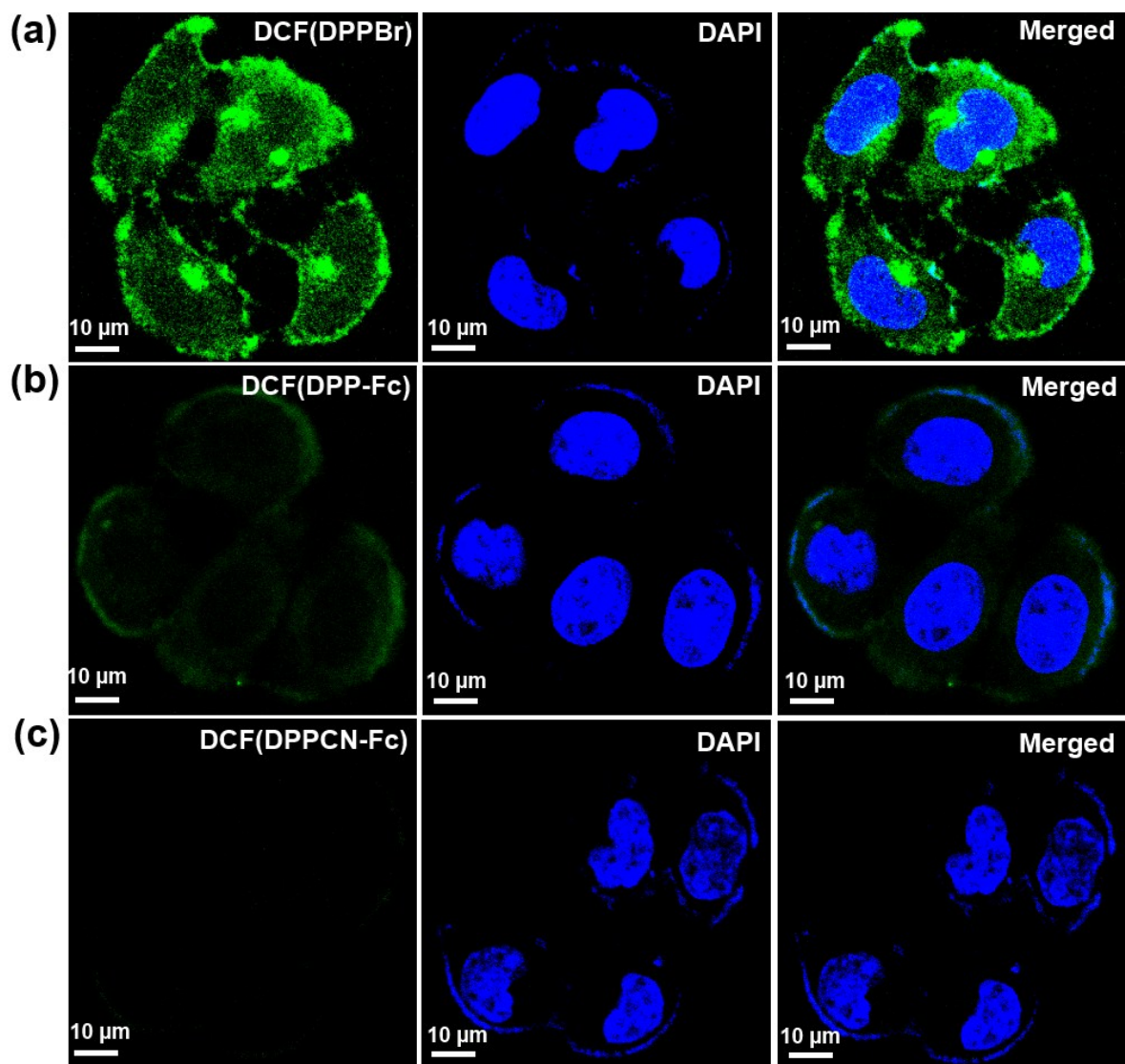


Figure S9. Fluorescence images of HeLa cells incubated with DPPBr, DPP-Fc, DPPCN-Fc under the existence of DCFH-DA. The green and blue colors represent the fluorescence images of DCF and DAPI, respectively.

Supplementary Information (SI)

Cell viability of A2780 cells

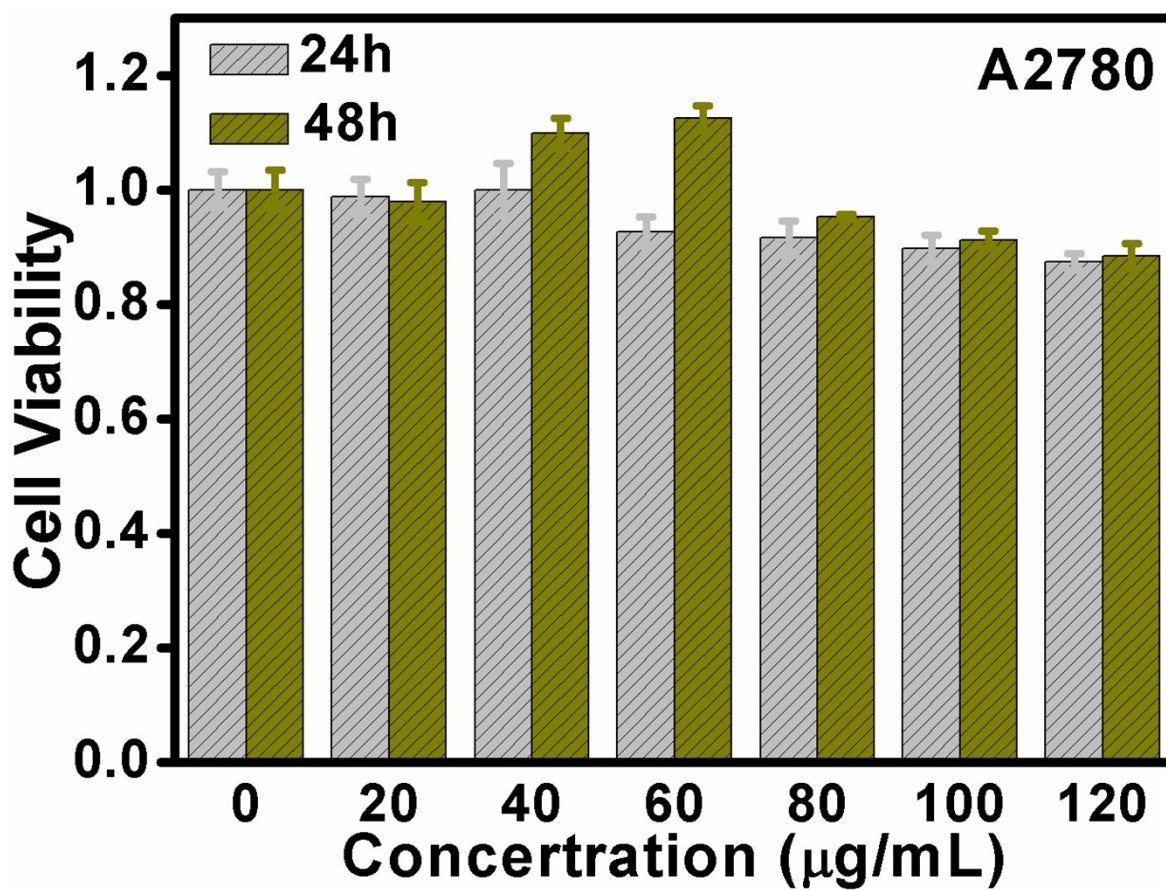


Figure S10. Cell viability of A2780 cells incubated with DPPCN-Fc NPs at different concentrations and time in dark condition.

Supplementary Information (SI)

H&E stained of major organs

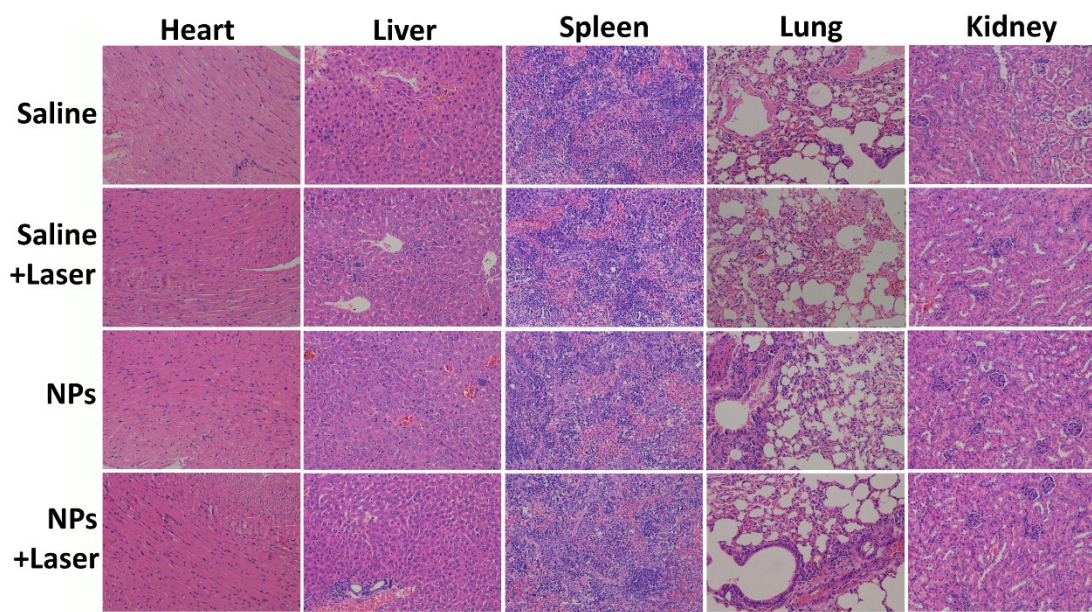


Figure S11. Photographs of H&E stained major organs including heart, liver, spleen, lung and kidney obtained from four groups after 18 days treatment.